Retinal Projection to the Pretectal Nucleus Lentiformis Mesencephali in Pigeons *(Columba Livia)*

Douglas R. Wylie,[1,2]* Jeffrey Kolominsky,[1] David J. Graham,[1] Thomas J. Lisney,[2] and Cristian Gutierrez-Ibanez[1]

[1]Centre for Neuroscience, University of Alberta, Edmonton, Alberta, Canada, T6G 2E9
[2]Department of Psychology, University of Alberta, Edmonton, Alberta, Canada, T6G 2E9

ABSTRACT

In birds, the nucleus of the basal optic root (nBOR) and the nucleus lentiformis mesencephali (LM) are retinal-recipient nuclei involved in the analysis of optic flow and the generation of the optokinetic response. The nBOR receives retinal input from displaced ganglion cells (DGCs), which are found at the margin of the inner nuclear and inner plexiform layers, rather than the ganglion cell layer. The LM receives afferents from retinal ganglion cells, but whether DGCs also project to LM remains unclear. To resolve this issue, we made small injections of retrograde tracer into LM and examined horizontal sections through the retina. For comparison, we also had cases with injections in nBOR, the optic tectum, and the anterior dorsolateral thalamus (the equivalent to the mammalian lateral geniculate nucleus). From all LM injections both retinal ganglion cells and DGCs were labeled. The percentage of DGCs, as a proportion of all labeled cells, varied from 2–28%, and these were not different in morphology or size compared to those labeled from nBOR, in which the proportion of DGCs was much higher (84–93%). DGCs were also labeled after injections into the anterior dorsolateral thalamus. The proportion was small (2–3%), and these DGCs were smaller in size than those projecting to the nBOR and LM. No DGCs were labeled from an injection in the optic tectum. Based on an analysis of size, we suggest that different populations of retinal ganglion cells are involved in the projections to LM, nBOR, the optic tectum, and the anterior dorsolateral thalamus. J. Comp. Neurol. 522:3928–3942, 2014.

INDEXING TERMS: displaced ganglion cells; retinal ganglion cells; optic flow; optokinetic; visual motion; optic tectum; anterior dorsolateral thalamus; nucleus of the basal optic root; accessory optic system; RRID:rid_000096

Optic flow, the motion that occurs across the entire retina during self-motion (Gibson, 1954), is analyzed in the vertebrate brain by retinal-recipient nuclei in the accessory optic system (AOS) and pretectum (for reviews, see Simpson, 1984; Simpson et al., 1988; Gamlin, 2006; Giolli et al., 2006). These nuclei are important for generating the optokinetic response to facilitate retinal image stabilization, without which both visual acuity and relative velocity discrimination are impaired (Westheimer and McKee, 1975; Nakayama, 1985). In birds, optic flow is processed by two retinal-recipient nuclei: the nucleus of the basal optic root (nBOR) of the accessory optic system (Karten et al., 1977), and the pretectal nucleus lentiformis mesencephali (LM) (Gamlin and Cohen, 1988). The visual response properties of both nuclei are highly similar. In both LM and nBOR, most neurons have large receptive fields in the contralateral visual field and exhibit direction-selectivity in response to largefield visual

Additional Supporting Information may be found in the online version of this article.

Grant sponsor: Natural Sciences and Engineering Research Council of Canada (NSERC) and the Canada Research Chairs Program (CRC) (to D.R.W.); Grant sponsor: NSERC Summer Undergraduate Research Award (to J.K.).

Present address for D.J. Graham: Lervig Aktiebryggeri, Vierveien 1 Hillevåg, 4016, Stavanger, Norway.

Present address for T.J. Lisney: Department of Psychology, Queen's University, Kingston, Ontario, Canada K7L 3N6.

Present address for C. Gutierez-banez: Lehrstuhl für Zoologie, Technische Universität München, Liesel-Beckmann Straβe 4 85354, Freising-Weihenstephan, Germany.

*CORRESPONDENCE TO: Douglas Wylie, Department of Psychology, University of Alberta, Edmonton, Alberta Canada T6G 2E9.
E-mail: dwylie@ualberta.ca

Received April 22, 2014; Revised July 2, 2014;
Accepted July 2, 2014.
DOI 10.1002/cne.23649
Published online July 2, 2014 in Wiley Online Library (wileyonlinelibrary.com)

motion (Burns and Wallman, 1981; Morgan and Frost, 1981; Gioanni et al., 1984; Winterson and Brauth, 1985).

Using injections of retrograde tracer into nBOR, studies have shown that the retinal input arises from the displaced ganglion cells (DGCs), which are found at the margin of the inner nuclear layer (INL) and inner plexiform layer (IPL), rather than the ganglion cell layer (Karten et al., 1977; Reiner et al., 1979; Fite et al., 1981). Given that the visual response properties are similar in LM and nBOR, a projection from the DGCs to the LM would not be surprising. However, there is some confusion in the literature in this regard. Fite et al. (1981), in a study of pigeon retinal projections, reported that one of their injections included the LM but retrogradely labeled DGCs were not observed. Bodnarenko et al. (1988) examined retinal labeling resulting from large injections of retrograde tracer in LM of chickens and concluded that DGCs did not project to LM. They found that retinal ganglion cells (RGCs) were retrogradely labeled from all injections, but DGCs were labeled only after injections that spread into the optic tract. Because the LM is located about 2 mm lateral to the nBOR (Karten and Hodos, 1967), it is unclear how the spread of an injection into the optic tract adjacent to the LM would label fibers of the basal optic root. Moreover, there are still statements in the literature indicating that DGCs project to the LM. For example, Woodson et al. (1995) cite unpublished observations (Karten and Mpodozis) that in pigeons, DGCs located in a horizontal band or "streak" project to LM. In the present study, to determine if DGCs project to LM, we made small injections of fluorescent retrograde tracers into LM and examined the labeling in the retina. As controls we also made injections in other retinal-recipient structures including nBOR, the optic tectum (TeO), and the anterior dorsolateral thalamus pars lateralis (DLL), which is part of the nucleus opticus principalis thalami (OPT), the avian homolog of the lateral geniculate nucleus (LGN) (Shimizu and Karten, 1993).

Abbreviations

AOS	Accessory optic system
CTB	Cholera toxin subunit B
DGC	Displaced ganglion cell
DLL/M	Anterior dorsolateral thalamus pars lateralis/medialis
GCL	Ganglion cell layer
GLv	Lateral geniculate nucleus, pars ventralis
GT	Tectal gray
III	Oculomotor nerve
INL	Inner nuclear layer
IPL	Inner plexiform layer
LGN	Lateral geniculate nucleus
LMm/l	Nucleus lentiformis mesencephali pars medialis/lateralis
LPC	Nucleus laminaris precommissuralis
MLd	Nucleus mesencephalicus lateralis, pars dorsalis
nBOR	Nucleus of the basal optic root
nRT	Nucleus rotundus
ONL	Outer nuclear layer
OPL	Outer plexiform layer
OPT	Nucleus opticus principalis thalami
RGC	Retinal ganglion cell
Ru	Red nucleus
SOp	Stratum opticum
SP	Nucleus subpretectalis
T	Nucleus triangularis
TeO	Optic tectum
TrO	Optic tract

MATERIALS AND METHODS

Surgery and tracer injection procedure

The methods reported herein conformed to the guidelines established by the Canadian Council on Animal Care and were approved by the Biosciences Animal Care and Use Committee at the University of Alberta. Eight pigeons (*Columba livia*), obtained from a local supplier, were anesthetized with an injection (i.m.) of a ketamine (65 mg/kg) / xylazine (8 mg/kg) cocktail. Supplemental doses were administered as necessary. Animals were placed in a stereotaxic device with pigeon ear bars and a beak bar adapter so that the orientation of the skull conformed to the atlas of Karten and Hodos (1967). A section of bone and dura was removed from the skull to allow access to LM, nBOR, TeO, and DLL on the left side of the brain with vertical penetrations through the brain using the stereotaxic coordinates. As outlined in Table 1, five of the birds received a single injection: three in LM (cases LM1, LM2, LM3), one in nBOR (case nBOR1), and one in DLL (case DLL1). The other three birds received two injections as indicated (cases LM/nBOR, LM/TeO, LM/DLL). For the injections into LM and nBOR, we recorded the activity of single units to moving largefield stimuli to ensure our placement in these nuclei. Extracellular recordings were made using glass micropipettes filled with 2 M NaCl, with tip diameters of 4–5 μm, which were advanced through the brain using a hydraulic microdrive (Frederick Haer, Millville, NJ). Extracellular signals were amplified, filtered, and fed to a window discriminator. Upon isolation of a unit in nBOR or LM, the direction preference of the unit was qualitatively determined by moving a large (90 × 90°) handheld visual stimulus, consisting of black bars, wavy lines, and dots on a white background, in the receptive field of the unit. With such stimuli LM and nBOR units can be easily identified (Wylie and Frost, 1990, 1996; Wylie and Crowder, 2000; Crowder and Wylie, 2001; Crowder et al., 2003a,b, 2004; Winship et al., 2006; Pakan et al., 2010). Once LM or nBOR was isolated, the recording electrode was replaced with a micropipette (tip diameter 20–30 μm) containing a fluorescent dextran; either micro-ruby (red) or micro-emerald (green) (3,000K molecular weight; Molecular Probes, Eugene, OR). To ensure we were at the correct location, recordings

TABLE 1.
Injections for All Cases

Case	Red injection(s)	Green injection(s)
LM1	LM *(dextran only)*	
LM2	LM (dextran + CTB)	
LM3		LM (dextran + CTB)
LM/nBOR	LM (dextran + CTB)	nBOR (dextran + CTB)
LM/DLL	DLL *(CTB only)*	LM (dextran + CTB)
LM/TeO	LM (dextran + CTB)	TeO (dextran + CTB)
nBOR1	nBOR (dextran + CTB)	
DLL1	DLL1(dextran + CTB)	

LM = lentiformis mesencephali; nBOR = nucleus of the basal optic root; DLL = anterior dorsolateral thalamus, pars lateralis; TeO = optic tectum.

were made of the visual responses with the dextran-containing micropipette prior to the injection. The dextran was iontophoretically injected (+4 μA, 1 second on, 1 second off) between 10 and 15 minutes. At the end of the injection period, the electrode was left undisturbed for 5 minutes, then withdrawn. Subsequently, a micropipette containing a fluorescent cholera toxin subunit B (CTB) of the same color as the BDA: either CTB-Alexa Fluor 488 (green) or 594 (red) conjugate (Molecular Probes) was inserted to the injection site. Recordings to visual stimuli were made to ensure we were at the correct location, and CTB was iontophoresed for 10–15 minutes (4 μA; 7 seconds on, 7 seconds off). Again, after the injection, the electrode was left undisturbed for 5 minutes, then withdrawn. This injection protocol was followed for all cases, with the following exceptions. In case LM1, only BDA was injected. In case LM/DLL, for the DLL injection, only CTB was injected. Finally, in case DLL1, in an effort to get a larger injection, ~0.05 μl of the CTB and BDA was pressure injected into DLL using a Picospritzer II (General Valve, Fairfield, NJ).

After the injections, the craniotomy was filled with bone wax, the wound was sutured, and the animals were given an i.m. injection of buprenorphine (0.012 mg/kg) as an analgesic. After a recovery period of 3 to 5 days the animals were deeply anesthetized with sodium pentobarbital (100 mg/kg) and immediately transcardially perfused with phosphate-buffered saline (PBS; 0.9% NaCl, 0.1 M phosphate buffer) followed by 4% paraformaldehyde in 0.1 M PBS (pH 7.4). The brain and the right eye were extracted from the skull and immersed in paraformaldehyde for several days at 4°C. The eye was hemisected along the limbus and the lens and vitreous were removed before the retina was dissected out of the overlying scleral eyecup. The brain and eye were then cryoprotected by placing them in 30% sucrose in 0.1 M PBS until they sank. Subsequently, they were embedded in gelatin and again cryoprotected in 30% sucrose in 0.1 M PBS overnight. Using a freezing stage microtome, the brain was sectioned in the coronal plane (40-μm thick) through the rostrocaudal extent of the injection sites and sections were stored in individual wells containing PBS. The entire retina was also sectioned on the microtome, but in the horizontal plane (40-μm thick sections). These sections were mounted on gelatinized glass slides, dried, and stored at 4°C. For those sections that were photographed, a blue nuclear stain was applied to visualize the retinal layers. A few drops of SlowFade Gold antifade reagent with DAPI (Invitrogen, Eugene, OR) were applied and the slides were coverslipped.

Because we were interested in obtaining a precise delineation of the injection sites in LM, and addressing the possible encroachment of the injections into the optic tract and other structures, once images of the injections were obtained (see below) the slides containing the LM injections were subsequently stained with thionine and coverslipped with Permount.

Microscopy and image analysis

Sections were viewed with a compound light microscope (Leica DMRE) equipped with the appropriate fluorescence filters (rhodamine and FITC). Images were acquired using a Retiga EXi FAST Cooled mono 12-bit camera (Qimaging, Burnaby, BC, Canada) and analyzed with OPENLAB imaging software (Improvision, Lexington, MA; RRID:rid_000096). Helicon Focus (Kiev, Ukraine) was used to bring stacks of images into focus, and panoramas were stitched together with PTGui (Rotterdam, Netherlands). Adobe Photoshop (San Jose, CA) was used to compensate for brightness and contrast. For retinal sections, the number of retrogradely labeled cells was counted from every fourth or eighth section (Table 2). Cells were classified as being RGCs or DGCs based on their location (Karten et al., 1977; Reiner et al., 1981; Fite et al., 1981). The cross-sectional areas of the RGCs and DGCs was measured from high-magnification photos using ImageJ (NIH, Bethesda, MD; http://rsb.info.nih.gov/ij/). For convenience we converted these to measures of diameters ($2 * \sqrt{area/\pi}$).

Nomenclature for LM

We used the nomenclature of the LM as outlined by Gamlin and Cohen (1988a,b). LM is divided into medial and lateral subdivisions (LMm and LMl). LMm is located rostromedial to LMl, and in Nissl sections the LMm appears slightly paler than LMl. At its lateral and caudal aspects, LMl is continuous with the rostral part of the

TABLE 2.

Number and Percentage of Retinal Ganglion Cells (RGCs) and Displaced Ganglion Cells (DGCs) Labeled From Each of the Injection Sites

	Case	RGCs (*n*:%)	DGCs (*n*:%)
Lentiformis mesencephali (LM)	LM1*	247 (99.2)	2 (0.8)
	LM2#	1474 (97.4)	39 (2.6)
	LM3*	109 (91.6)	10 (8.4)
	LM/nBOR#	2634 (98.6)	37 (1.4)
	LM/DLL#	134 (72.0)	52 (28.0)
	LM/TeO#	2062 (98.2)	37 (1.8)
	Mean percentage ± SD	(92.8 ± 10.6)	(7.2 ± 10.6)
Nucleus of the basal optic root (nBOR)	LM/nBOR#	23 (6.8)	313 (93.2)
	nBOR1*	72 (16.1)	376 (83.9)
	Mean percentage ± SD	(11.5 ± 6.6)	(88.5 ± 6.6)
Anterior dorsolateral thalamus, pars lateralis (DLL)	LM/DLL#	116 (98.3)	2 (1.7)
	DLL1#	1312 (97.2)	38 (2.8)
	Mean percentage ± SD	(97.8 ± 0.8)	(2.2 ± 0.8)
Optic tectum (TeO)	LM/TeO#	330 (100)	0 (0)

The counts were obtained from the examination of every fourth* or every eighth# serial section through each retina.

tectal gray (GT), which contains mainly small cells and appears continuous with layer 5 of the TeO in Nissl-stained sections. LMm, LMl, and the GT all receive retinal input (Gamlin and Cohen, 1988). LMm is bordered medially by the nucleus laminaris precommissuralis (LPC), a thin strip of cells that stains dark in Nissl sections. LPC does not receive retinal input.

RESULTS

Injection sites

The data reported are based on 11 injections in 8 birds, as outlined in Table 1. As the focus of the study was the retinal projection to LM, there were six injections in LM. In addition, there were two injections in nBOR, two in DLL, and one in TeO. Figure 1 shows photomicrographs of the LM injection site from case LM/DLL. Two sections are shown, 160 μm apart. Figure 1A shows a higher magnification photomicrograph of the injection from the more rostral section. A lower magnification photomicrograph of the same section stained for thionine is shown in Figure 1B, with the injection pasted on top. Similarly, Figure 1C shows the more caudal section stained for thionine, with the green fluorescent injection. A more detailed description is offered below. Figure 1 also shows injection sites in TeO, nBOR, and DLL. The TeO injection (Fig. 1D) was small, about 200 μm in diameter, and confined to the superficial retinorecipient layers. The nBOR injection shown (Fig. 1F) is from case nBOR1. This injection was confined to the lateral margin in the rostral half of the nucleus and was about 200 μm in diameter. The nBOR injection from case LM/nBOR (not shown) was quite similar. It was about the same size and located in the lateral margin of nBOR but slightly more caudal than in case nBOR1. The DLL injection shown (Fig. 1E) is from case DLL1. Centered appropriately above the nucleus rotundus (nRT), it was quite large. It extended into other structures including nRT and nucleus triangularis (T). It may have also spread medially to the anterior dorsolateral thalamus pars medialis (DLM) and dorsally into the septomesencephalic tract and the nucleus superficialis parvocellularis. Critically, the injection did not spread laterally into pretectal regions, TeO, or the optic tract. Thus, the only retinal recipient area included in this injection was DLL. The DLL injection from case LM/DLL (not shown) was very small. It was located right on the border of nRT and DLL. It was confined to the ventral DLL and the dorsal 100 μm of nRT.

We reconstructed all six of the LM injections. Drawings of the injection sites, with the borders determined from Nissl-stained sections, are shown in Figure 2. Four serial sections, from caudal (left) to rostral (right) are shown for each case. The sections are 160 μm apart with the exception of case LM3, where 80 μm intervals are shown because the injection was quite small. LMl and LMm are shown as shaded yellow and blue, respectively, and the injections are shaded red. Note that for the sections in case LM/DLL (U-X), Figure 2V,W are drawings of the photomicrographs shown in Figures 1C and 1B, respectively. We were very liberal with our estimates of the size of the injections in LM to address the possibility that tracer may have spread to the optic tract.

For case LM1 (Fig. 2A–D), the heart of the injection was concentrated rostrally in LMm (Fig. 2D). In more caudal sections the injection appeared less intense and straddled the LMm/l border (Fig. 2B,C). It is possible that there was some spread of the injection into the optic tract but this would be minimal (Fig. 2D). The

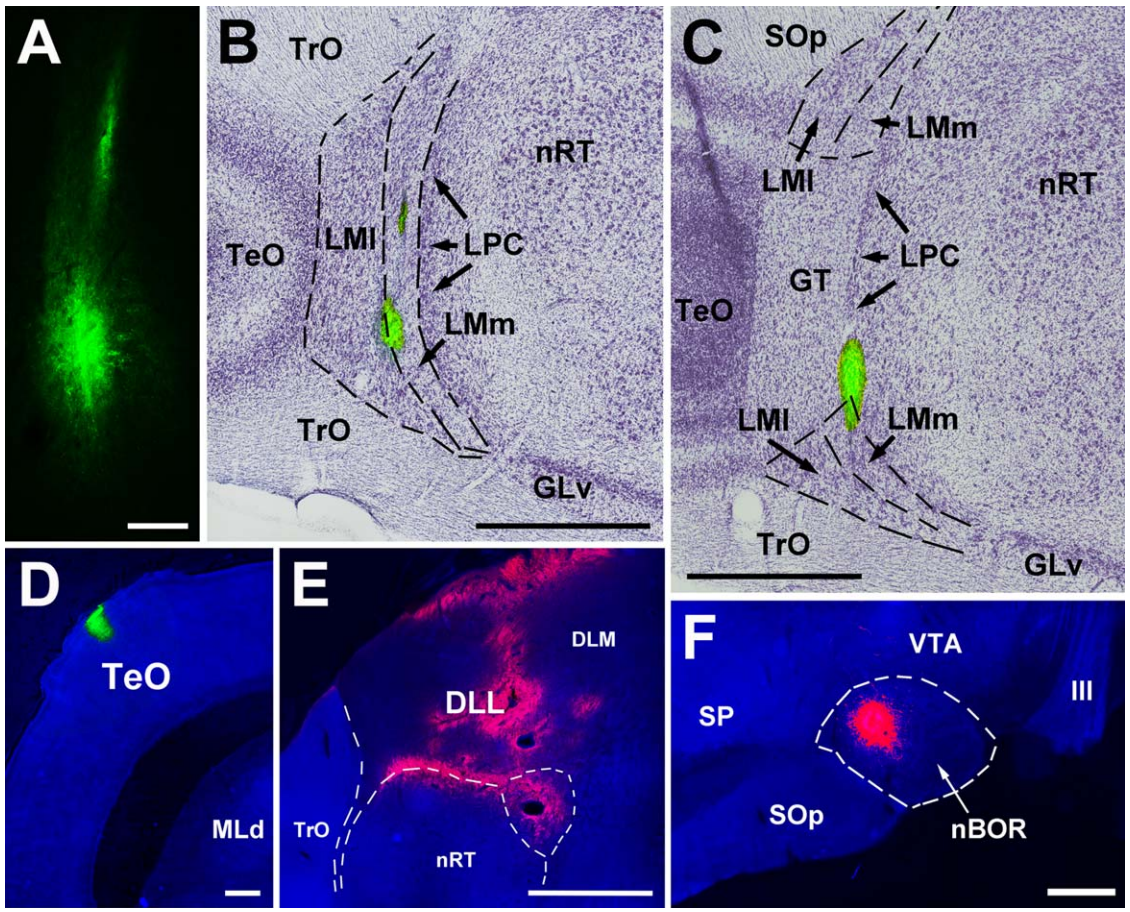

Figure 1. Photomicrographs of injection sites. **A–C:** The injection in the lentiformis mesencephali (LM) from case LM/DLL. Two sections, 160 μm apart, are shown. A shows the green fluorescent injection site from the more rostral of the sections. In B, this injection is superimposed on the Nissl-stained section. Similarly, C shows the injection from the more caudal section. In the more rostral section (A,B) the injection was on the border of the medial and lateral subnuclei of LM (LMm, LMl) with a little leakage of tracer along the electrode track in LMm. The more caudal section (C) shows that the injection spread slightly into the nucleus laminaris precommissuralis (LPC) and the tectal gray (GT). **D–F:** Respectively show injections in the optic tectum (TeO) (case LM/TeO), anterior dorsolateral thalamus pars lateralis (case DLL1), and nucleus of the basal optic root (nBOR) (case nBOR1) . Scale bars = 200 μm in A; 1 mm in B,C; 400 μm in D; 500 μm in E,F.

injection in case LM2 was larger and concentrated in the ventral part of LMl (Fig. 2G). In more rostral sections, the main part of the injection included LMm, and there was apparent spread of the injection along the injection electrode into more dorsal parts of LMm and the LPC (Fig. 2G,H). This spread touched the dorsal margin of LMl (Fig. 2H) but the optic tract was spared. The injection in case LM3 (Fig. 2I–L) was quite small. It was found rostrally, spanning the LMm/l border (Fig. 2J,K), but did not extend outside LM. For case LM/nBOR (Fig. 2M–P) the LM injection was concentrated at the mid and ventral levels of LMl (Fig. 2N,O). There was perhaps some spread to LMm and the optic tract (Fig. 2P). This included what appeared to be a small, faint deposit of tracer just ventral to LM (Fig. 2O). Case LM/TeO (Fig. 2Q–T) was the only case where the LM injection clearly spread into the optic tract. The injection was large and concentrated in ventral LMl but spread into the LMm (Fig. 2Q,S). At the heart of the injection site, there was clear spread ventrally into the optic tract (Fig. 2R). In case LM/DLL, the LM injection was quite small. It was concentrated caudoventrally along the border of LMl and LMm (Figs. 2W and 1A,B). More of the injection was in LMm compared to LMl. More caudally, the injection appeared to spread into the adjacent LPC and perhaps the GT (Figs. 2V and 1C).

From all the LM, nBOR, and DLL injections, both DGCs and RGCs were labeled. From the TeO injection, RGCs were labeled, but no DGCs were labeled. The retinal labeling from each of the structures will be presented in turn below with reference to Figures 3–5 and Table 2. Figures 3 and 4 show photomicrographs of retrogradely labeled DGCs and RGCs. Figure 5 shows the distribution of labeled RGCs and DGCs on the retina.

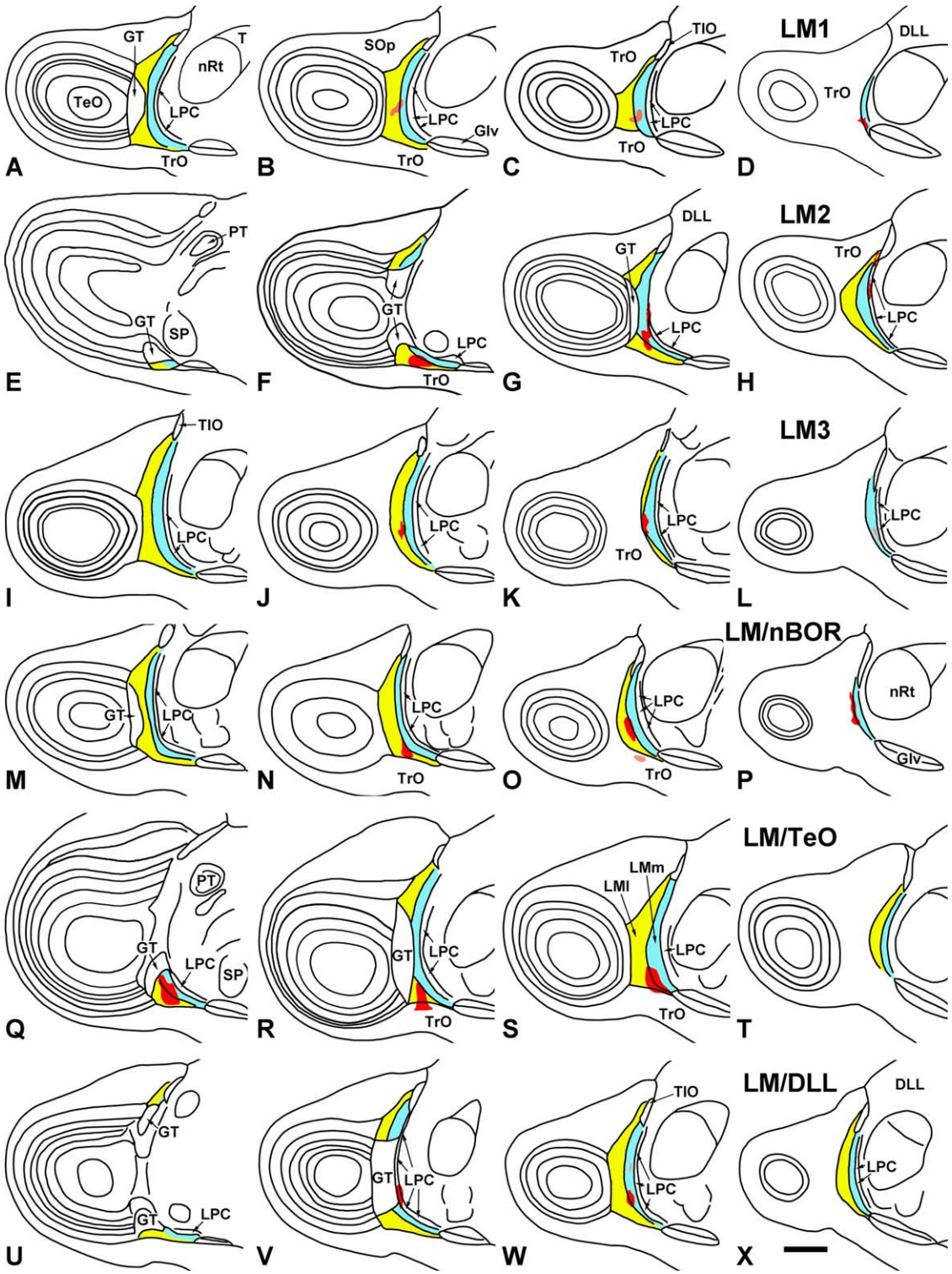

Figure 2. Drawings of serial sections through the pretectum showing the injection sites in the nucleus lentiformis mesencephali (LM) for all six cases involving injections in LM. The sections run from caudal (left) to rostral (right). The medial and lateral subnuclei of LM (LMm, LMl) have been shaded light blue and yellow, respectively, and the injections are indicated with red-shaded regions. Lighter red regions appear in **B,C,K,L,X**, indicating that these injection sites were not as intense. With the exception of case LM3 (**I–L**) the sections are 160 μm apart in the coronal plane. For case LM3, sections that were 80 μm apart are shown because the injection was so small. For other abbreviations, see list. Scale bar = 1 mm.

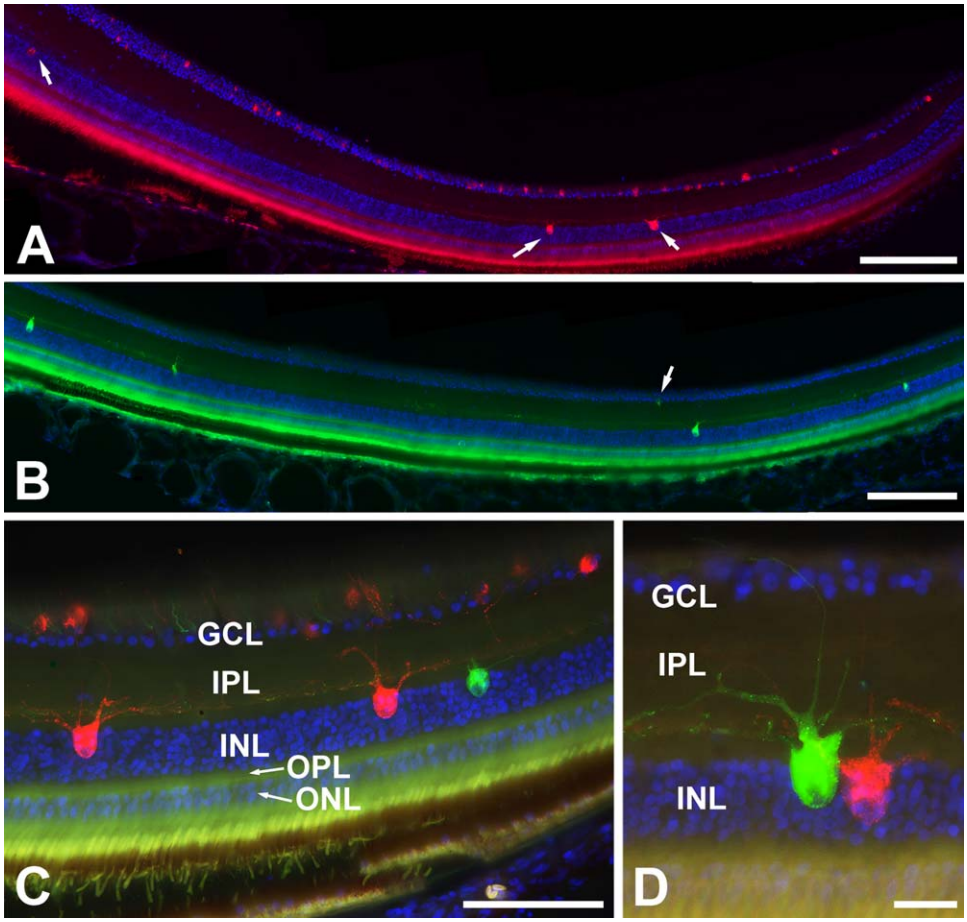

Figure 3. Retrogradely labeled retinal ganglion cells (RGCs) and displaced ganglion cells (DGCs) from case LM/nBOR, in which red tracer was injected in lentiformis mesencephali (LM) and green tracer was injected in the nucleus of the basal optic root (nBOR). A blue nuclear stain has been used to clearly visualize the layers of the retinae. **A:** Cells retrogradely labeled from the LM injection. Although most labeled cells were RGCs found in the ganglion cell layer (GCL), a few DGCs, indicated by the white arrows, were found straddling the inner nuclear layer (INL) and inner plexiform layer (IPL). **B:** Retrogradely labeled cells from the injection of green tracer in the nBOR. Although most labeled cells were DGCs, an RGC is also apparent (white arrow). **C,D:** Higher-magnification photomicrographs of retrogradely labeled cells. Note that the red and green DGCs are quite similar with respect to morphology and orientation, with dendrites extending into, and traveling horizontally within, the IPL. (The supplementary figure provided shows a green-magenta version of this figure). For other abbreviations, see list. Scale bars = 200 μm in A,B; 100 μm in C; 25 μm in D.

Table 2 shows the number of RGCs and DGCs labeled for each injection as counted from either every fourth or eighth section as indicated.

Retinal labeling from LM injections

From the LM injections, although mostly RGCs were labeled (Figs. 3A-C, 4A,B), DGCs were labeled in all cases (Figs. 3A,C,D, 4A,C) (Table 2). In case LM1, there was a focus of retrogradely labeled RGCs just temporal to the central retina, dorsal to the pecten (Fig. 5A). A few other RGCs were found medial and lateral to this, such that the overall pattern tended towards a streak. Few DGCs were labeled in this case (0.8%), but they were found in the temporal region of the heart of the distribution of labeled RGCs. In case LM2, the distribution of retrogradely labeled cells was much more extensive (Fig. 5B). There was a concentration of RGCs in the dorsocentral retina including the ventral half of the red field, but they were also found in the ventronasal retina, and a small number were found in the ventrotemporal retina. Compared to case LM1, more DGCs were labeled (2.6%), and most of these were found in the dorsotemporal retina, with fewer in the nasal retina. The least amount of retrograde labeling was seen in case LM3, which had the smallest injection, although a more substantial proportion of the labeling was DGCs (8.4%). The retrogradely labeled cells were found along a near horizontal streak extending from the central retina to the temporal edge (Fig. 5C). Whereas the RGCs were concentrated in the central retina, the DGCs were

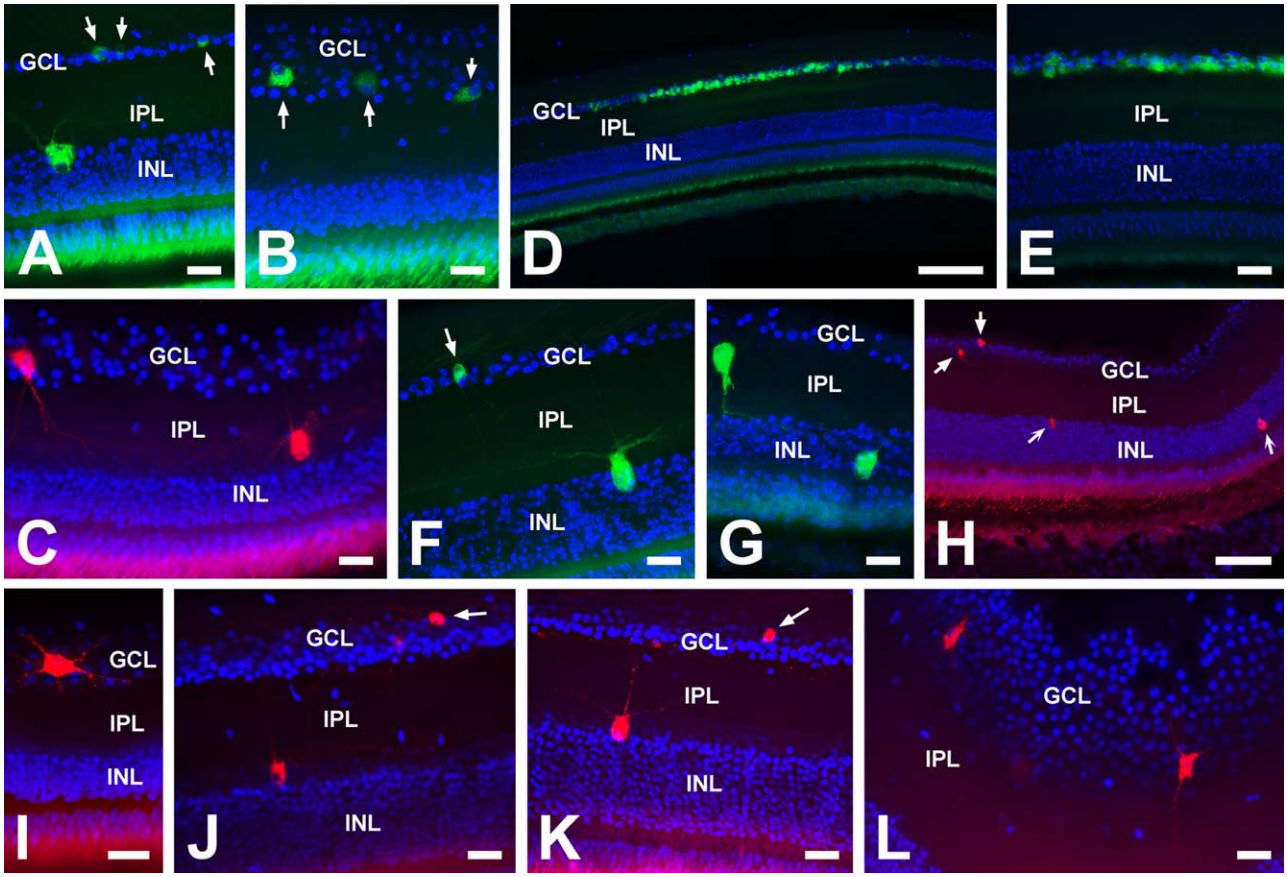

Figure 4. Retrogradely labeled retinal ganglion cells (RGCs) and displaced ganglion cells (DGCs). A blue nuclear stain has been used to clearly visualize the layers of the retinae. **A–C:** Retrogradely labeled RGCs and DGCs from injections in the lentiformis mesencephali (LM). Most of the RGCs were small (A), although some larger ones were seen (B). The largest labeled RGCs approached the size of the DGCs (C). **D–E:** Tightly clustered small RGCs labeled from the injection in the optic tectum (TeO). **F–G:** Retrogradely labeled RGCs and DGCs from injections in the nucleus of the basal optic root (nBOR). Although some of the RGCs were small (F), most were large (G). **H–L:** RGCs and DGCs labeled from an injection in the anterior dorsolateral thalamus pars lateralis (DLL). The RGCs labeled were on average larger than those labeled from injection in LM and TeO (I,L), whereas the DGCs were smaller than those labeled from injections in LM and nBOR (**J,K**). The white arrows highlight RGCs, with the exception of the two stylized arrows in H, which indicate DGCs. For other abbreviations, see list. Scale bars = 25 μm in A–C, E–G, I–L; 200 μm in D; 100 μm in H.

found in a small cluster in the temporal retina. The retrograde labeling from the LM injections for cases LM/nBOR and LM/TeO were quite similar to one another (Fig. 5D,E). A rather thick horizontal streak of cells was labeled in both cases. The streaks were located along and just ventral to the center of the retina and spanned from the temporal edge to about halfway into the nasal half of the retina. That is, the nasal-most quarter of the retina was spared. For both cases, most of the labeled DGCs were found in the temporal retina and a similar percentage of DGCs was labeled in both cases (1.4 and 1.8%). For the LM injection in case LM/DLL, the retrograde labeling was found in a horizontal streak from the central retina to the temporal edge (Fig. 5F). This case had, by far, the greatest proportion of DGCs (28%), which were distributed in the same region as the RGCs.

In summary, from the injections of LM, retrogradely labeled RGCs were usually observed as a horizontal streak. This streak was along or near the horizontal meridian and extended more so temporally than nasally. DGCs were labeled in all cases, but the percentage of retrogradely labeled cells that were DGCs varied considerably from $<1\%$ to 28% (average $\pm$ SD $= 7.2 \pm 10.6$). Overall, most of the labeled DGCs were found in the temporal retina near the horizontal meridian.

Retinal labeling from nBOR injections

The pattern of retrograde labeling in the retina was similar from the two nBOR injections. Most of the labeling was of DGCs (proportion = 84–93%), although some RGCs were labeled (Figs. 3B–D, 4F,G). The proportion of labeled RGCs was higher for case nBOR1 compared

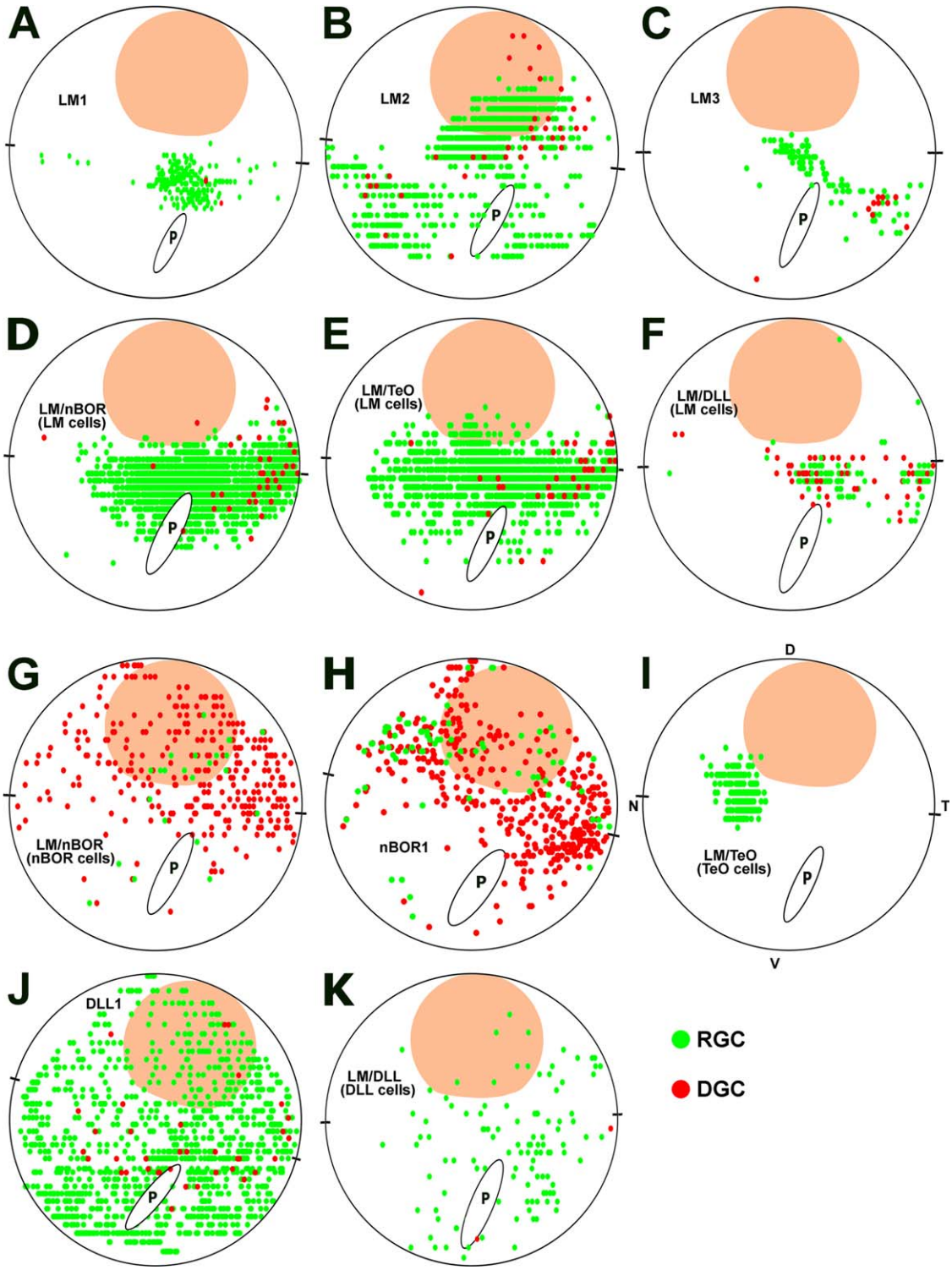

Figure 5. Fig. 5. Distributions of retrogradely labeled retinal ganglion cells (RGCs; green) and displaced ganglion cells (DGCs; red) for all cases. These were reconstructed from horizontal sections through the retina, 320 μm apart (**B,D–G,I–K**) or 160 μm apart (**A,C,H**). Data from the six LM injections are shown in A–F. The ellipsoid in the ventral retinal indicates the pecten (P) and the shaded circle in the dorsal retina represents the red field, approximated based on figures from Nalbach et al. (1990) and Hayes and Holden (1983). The two dashes intersecting each circle denote the horizontal plane. This was established based on the orientation of the pecten relative to the horizontal, from the figures in Hayes and Holden (1983). N = nasal; T = temporal; V = ventral; D = dorsal.

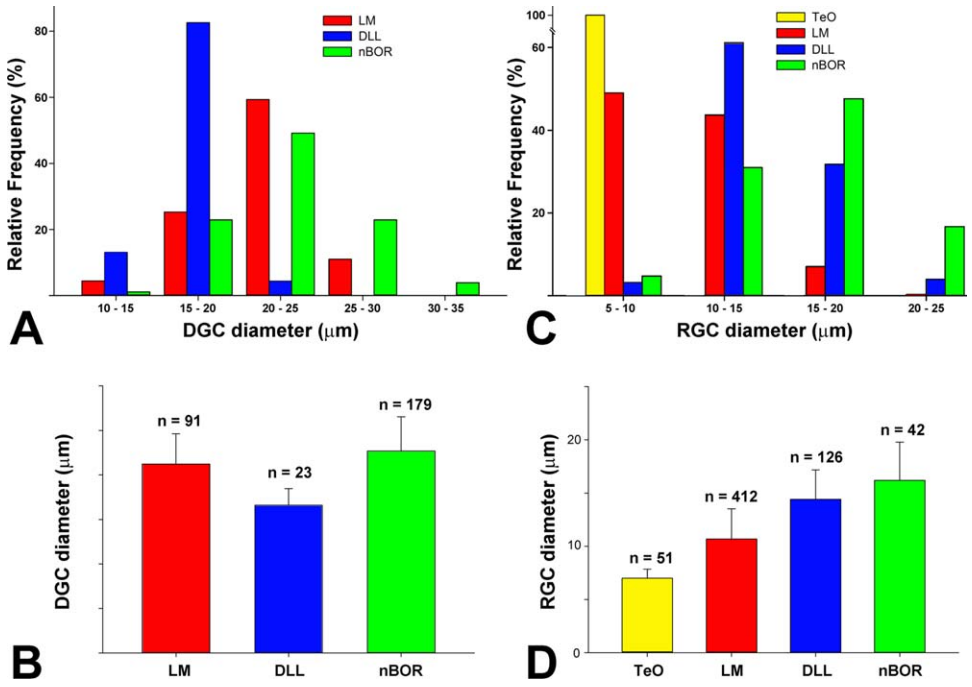

Figure 6. Relative sizes of the displaced ganglion cells (DGCs) (**A,B**) and retinal ganglion cells (RGCs) (**C,D**) projecting to the lentiformis mesencephali (LM; red), nucleus of the basal optic root (nBOR; green), anterior dorsolateral thalamus pars lateralis (DLL; blue), and the optic tectum (TeO; yellow). On the top (A,C) frequency histograms are shown. The frequency is expressed as a percentage for each group as a function of cell diameter in 5-μm increments. On the bottom (B,D) the mean diameter for each group is shown. Error bars represent 1 SD. The number in each sample is also indicated above the error bars.

to LM/nBOR (16.1% vs. 6.8%). Compared to the LM injections, the DGCs from the nBOR injections were distributed across the retina but scarce in the ventronasal region (Fig. 5G,H). The greatest density of DGCs was in the temporal retina, particularly in case nBOR1. The density of RGCs was higher in the dorsonasal retina for case nBOR1, but in case nBOR/LM the RGCs were scattered in the dorsotemporal retina.

Retinal labeling from the TeO injection

The TeO injection resulted in a cluster of RGCs along the horizontal meridian in the nasal retina (Fig. 5I). This cluster of RGCs was tightly packed to the point that the borders of the individual of individual RGCs could be difficult to determine (Fig. 4D,E). The density of the RGCs was greater than that from the LM injections (e.g., Figs. 3C, 4A,B).

Retinal labeling from DLL injections

From the two DLL injections, both RGCs and DGCs were labeled. Despite a large difference in the amount of retrograde labeling, the distribution across the retina was similar. For case DLL1, RGCs were found throughout the retina, although clearly more were seen in the temporal and ventral parts of the retina (Fig. 5J). In case LM/DLL much less labeling was seen, with RGCs scattered throughout the temporal two-thirds of the retina, and the density was greatest in the ventrotemporal retina (Fig. 5K). Note that from this small localized injection in DLL, the RGCs were scattered, not clustered as observed with the TeO injection (e.g., Fig. 5I). DGCs were labeled from the both DLL injections (proportion = 2.8%, 1.7%) and like the RGCs, most were found in the ventrotemporal retina.

Comparison of DGC sizes

As outlined in Table 2, DGCs were labeled from all injections in LM, nBOR, and DLL. They were larger than the RGCs, ranging from 11–34 μm in diameter. Figure 6A shows a frequency histogram of DGC diameter for those labeled from injections in LM, DLL, and nBOR. A histogram showing the mean diameters for all three groups is shown in Figure 6B. Analysis of variance (ANOVA) revealed a significant difference between the groups ($F(2, 290) = 31.16$, $P \ll 0.001$). Post-hoc *t*-tests revealed that all three groups were different from one another (all $P < 0.002$). Those DGCs labeled from DLL injections were clearly smaller than those labeled from LM and nBOR injections (see Figs. 4J,K vs. 3C,D and 4A,C). Most of the DGCs labeled from DLL injections were 15–20 μm in diameter (mean ± SD = 16.6 ± 1.86 μm), whereas

most labeled from the nBOR and LM injections were 20–25 μm in diameter (LM = 21.2 ± 3.42 μm, nBOR = 22.7 ± 3.84 μm; mean ± SD). Otherwise the morphology of the DGCs that project to DLL did not appear appreciably different. Most were observed to be straddling the INL/IPL border with dendrites extending into and traversing laterally within the IPL. The cell bodies were ovoid with an aspect ratio of about 2:1 and oriented with the long axis perpendicular to the retinal layers. Although the distributions for the DGCs projecting to the nBOR and LM were largely overlapping (Fig. 6A), and the means differed by less than 10%, the nBOR-projecting DGCs were significantly larger (*t*-test, $P < 0.002$). As can be seen in the frequency histogram (Fig. 6A), this was due to the fact that most of the largest DGCs (>25 μm in diameter) were labeled from nBOR injections. Otherwise the LM- and nBOR-projecting DGCs looked highly similar (Figs. 3C,D, 4A,C,F,G).

Comparison of RGC sizes

RGCs were labeled from all injections, and there were some obvious differences with respect to the sizes of those labeled from injections in LM, nBOR, TeO, and DLL. Figure 6C shows a frequency of RGC diameter for those labeled from injections in LM, DLL, TeO and nBOR. The diameter was quite variable, ranging from 5–25 μm. The mean diameters for all groups are shown in Figure 6D. An ANOVA revealed a significant difference between the groups ($F(3, 627) = 148.61$, $P \ll 0.001$). Post-hoc *t*-tests revealed that all four groups were different from one another (all $P < 0.005$). Those labeled from TeO were the smallest and showed the least variability (diameter = 6.81 ± 0.9 μm; mean ± SD) (see Fig. 4E). The LM-projecting RGCs were bigger on average (diameter = 10.61 ± 2.84 μm; mean ± SD), but showed more variability. While most (49%) were as small as the TeO-projecting RGCs and in the 5–10 μm bin (Fig. 4A), there were many LM-projecting RGCs with diameters in the 10–15 μm range (Figs. 4B, 6C), and some even larger RGCs approaching the size of the DGCs (Fig. 4C). The DLL-projecting RGCs were even larger, averaging 14.42 ± 2.70 μm in diameter (mean ± SD). Most (61%) were in the 10–15 μm range (Fig. 4J–L) and a few very large RGCs were observed (Fig. 4I). The RGCs labeled from the nBOR injections were the largest (diameter = 16.21 ± 3.58 μm; mean ± SD). Although a few small RGCs were observed (Fig. 4F), most (48%) were found in the 10–15 μm range (Fig. 6C). 17% of the nBOR-projecting RGCs were as large as the DGCs (20–25 μm range) (Figs. 4G, 6C).

DISCUSSION

DGCs project to the LM, nBOR, and DLL

In this report we have shown that DGCs project to the LM in pigeons. Most of the retrogradely labeled cells were RGCs, but DGCs were labeled from all six injections in LM. The proportion of DGCs expressed as a percentage of total labeled cells varied considerably, from 0.8 to 28% (mean = 7.2%). The labeling of the DGCs is not likely due to the spread of the retrograde tracer into the optic tract, as was concluded by Bodnarenko et al. (1988). Although some of our LM injections did encroach upon the optic tract (e.g., cases LM/nBOR and LM/TeO), most of the injections were quite small and confined to LM (Fig. 2). Moreover, the injections that did encroach upon the LM did not result in a greater percentage of labeled DGCs. In fact, the two LM injections, which resulted in the largest proportion of labeled DGCs (cases LM3 [8.4%] and LM/DLL [28%]), were among the smaller of the injections. It is not clear why these injections resulted in relatively more labeling of DGCs. Both were located on the LMm/l border but may have involved more of the LMm. With perhaps the exception of case LM1, in the other cases the injection involved more of the LMl.

Woodson et al. (1995) noted that there was a discrepancy between the number of DGCs labeled from injections in the nBOR of pigeons (4,800; Fite et al., 1981) and the total number of DGCs, which was estimated to be as many as 6,000 by Binggeli and Paule (1969) from stained cross-sections of the pigeon retina. Woodson et al. (1995) suggested the difference was due to the fact that some DGCs project to the LM. We would further add that the discrepancy is due to the fact that some DGCs project to DLL.

Do different DGCs project to the LM, nBOR, and DLL?

It has been previously been shown that the avian nBOR receives the bulk of its retinal input from DGCs (Karten et al., 1977; Fite et al., 1977; Reiner et al., 1979). Fite et al. (1981) noted that from large injections covering most of the nBOR in pigeons, labeling was heaviest in the inferior-temporal and temporal regions of the retina, but less dense in the inferior nasal retina and red field. In both of our nBOR injections, which were smaller and located in the lateral half of the nucleus (Fig. 1F), labeling was heaviest in the temporal retina. With case nBOR1 there was a paucity of labeling in the dorsal part of the red field and the amount of labeling in the ventral retina was less than that observed by Fite et al. (1981). Given that in the present study the nBOR injections were small and confined to the lateral nBOR, it is possible that there is a coarse topography in the retinal projection to nBOR such that the inferior retina is represented more medially. Nonetheless, it should be noted that even small

injections in nBOR resulted in labeling of DGCs spread across large parts of the retina.

From the LM injections, however, DGCs were not found throughout the retina. In all cases, most of the labeled DGCs were found in the temporal half of the retina. In four of the cases (LM3, LM/nBOR, LM/TeO, LM/DLL) this labeling was restricted to the temporal retina near the horizontal meridian. Hayes and Holden (1983) plotted the distribution of DGCs in the pigeon retina. DGCs had two areas of peak density: the fovea and a temporal region along the horizontal meridian. It seems that this temporal region of high DGC density provides input to LM. Case LM2 was the oddball with respect to DGC distribution, as there were loose clusters in the dorsotemporal and ventronasal regions of the retina. This case also had the largest injection site and was the only injection that encroached upon the dorsal LM. Taken together, our data suggest that there might be a retinotopy with the DGC projection to LM. This retinotopy is discussed below in more detail with respect to RGC labeling.

We observed that DGCs were also labeled from both of our injections in the DLL, although their proportion relative to RGCs was small (1.7% and 2.8% in cases LM/DLL and DLL1, respectively). Retrograde labeling of DGCs from injections in the principal optic nucleus of the thalamus (OPT), which includes DLL, was not noted by Remy and Gunturkun (1991) or Miceli et al. (2006). However, both of these studies examined wholemounts of the retina; thus, it would have been difficult to ascertain the presence of DGCs, particularly given their scarcity. The DLL-projecting DGCs were clearly smaller than those labeled from LM and nBOR injections (Fig. 6A,B), suggesting that a different class of DGC projects to the DLL. Although the LM- and nBOR-projecting DGCs looked highly similar (Fig. 3D), the latter were slightly larger, as there were some extremely large DGCs (>25 μm diameter) that were labeled from nBOR injections (Fig. 6A).

There have been reports of different classes of DGCs in the pigeon retina based on immunochemistry. Most of these studies used retrograde transport from the nBOR combined with immunohistochemistry and as such one can only offer speculation as to those DGCs projecting to DLL and LM. In a series of studies, Britto and colleagues (Britto et al., 1988; Britto and Hamassaki, 1991; Britto and Hamassaki-Britto, 1993) retrogradely labeled DGCs by injection of tracer into nBOR, and examined immunoreactivity to tyrosine hydroxylase, enkephalin, substance P, and cholecystokinin. Only 9–25% of the retrogradely labeled DGCs showed immunoreactivity to any one of these four antigens. Enkephalin and tyrosine hydroxylase immunoreactivity was observed in small DGCs, 10–16 μm in diameter. Most of the DGCs showing substance P immunoreactivity were 14–20 μm in diameter, and most of those expressing cholecystokinin were 18–26 μm in diameter. From the data in the present study we would conclude that the cholecystokinin immunoreactive DGCs are not likely involved in the projection to the DLL. Based on their size, all of these types of DGCs may project to the LM. A few studies of the chicken retina are also relevant to this discussion. Wilson et al. (2011) found that about two-thirds of the DGCs were nitriergic (see also Fischer and Stell, 1999). These DGCs had cell bodies >20 μm in diameter, typical of the nBOR- and LM-projecting DGCs. Finally, Nickla et al. (1994) found that the large DGCs projecting to nBOR expressed cytochrome oxidase. In summary, these aforementioned immunohistochemical studies have revealed that there are different classes of DGCs with respect to neurochemical contribution and size. As we have shown that the DGCs projecting to DLL, nBOR, and LM differ with respect to size, it is likely that these projections have differing neurochemical footprints.

Different RGCs project to the LM, nBOR, and DLL

RGCs were retrogradely labeled from all injections in this study. From the TeO, a cluster of densely packed RGCs was labeled, consistent with the tight retinotopy of this projection (e.g., Clarke and Whitteridge, 1976). The TeO-projecting RGCs were all very small, with an average diameter of 6.8 μm. This confirms the findings of Remy and Gunturkun (1991), who reported the average diameter of TeO-projecting RGCs to be 7.5 μm. Also consistent with the present study, Remy and Gunturkun (1991) found that injections in the OPT (including DLL) resulted in no clear retinal topography, but rather RGCs were found throughout the retina at a low density. They noted that most (70%) of the OPT-projecting RGCs had diameters between 8–14 μm (mean = 11.7 μm). Our measurements of the DLL-projecting RGCs were similar, as most (61%) had diameters in the 10–15 μm range, although the mean was slightly higher (14.4 μm). As discussed by Remy and Gunturkun (1991), it has been noted in other birds (Bravo and Pettigrew, 1981) that only large and medium-sized RGCs project to the OPT, whereas a heterogeneous group of RGCs encompassing all sizes project to the TeO, suggesting a separation of function.

From the LM injections, mostly small RGCs were labeled (5–10 μm), but larger (up to 20 μm) RGCs were also labeled. (Only one was >20 μm in diameter; Fig. 6C.) This is similar to what Bodnarenko et al. (1988) reported for LM-projecting RGCs in the chicken, but the cells were larger on average. The size range they reported was 25–840 μm^2 (5.6–32 μm diameter).

They noted that most cells were small, but the mean size (area = 230 μm^2, diameter = 17.1 μm) was somewhat higher than we observed (10.6 μm diameter). This could be due to a species difference, or the fact that Bodnarenko et al. (1988) used a different nomenclature for the LM, where GT is included as part of LM. The GT is retino-recipient (Gamlin and Cohen, 1988) and perhaps this projection arises from very large RGCs.

Retinotopy in LM?

In their study of the retinal projection to the chicken LM, Bodnarenko et al. (1988) showed a topographic projection to the LM as a whole, which included LMl, LMm, and GT. From their injections in LM, generally a horizontally streak of RGCs extending across the retina was labeled, much like we observed in most of our cases (Fig. 5A,C–F). They found that the location of this streak of DGCs varied depending on the location of the injection, such that the inferior-superior axis of the retina was represented along the dorsal-ventral axis in LM, and the temporal-nasal axis of the retina was represented along the rostrocaudal axis in LM. Gamlin and Cohen (1988) proposed a different retinotopy for the pigeon LM based on injections of anterograde tracer in small areas of the retina. In their scheme, LMm and LMl have separate retinotopic maps that are mirror images as reflected about a vertical axis. The dorsal, ventral, nasal, and temporal quadrants of the retina are represented, respectively, in the ventrolateral, dorsomedial, dorsolateral, and ventromedial regions of LMl, and the ventromedial, dorsolateral, dorsomedial, and ventrolateral regions of LMm.

We have used these data from Gamlin and Cohen (1988) and offer an approximation of the retinotpic map in LMl and LMm, as shown in Figure 7 in order to determine if our results validate those of Gamlin and Cohen (1988). In case LM1, the injection was right on the border of LMl and LMm just below the middle of the dorsoventral extent (Fig. 2A–D). That the retrograde labeling was found just temporal and ventral to the center of the retina is consistent with the proposed retinotopy. In cases LM3 and LM/DLL, the injections were along the border of LMm and LMl but clearly below the middle of the dorsoventral extent (Fig. 2J,K,X). The retrograde labeling was found in the temporal retina just ventral to the horizontal meridian (Fig. 5C,F). Because the medial edge of the LMl and the lateral edge of the LMl represent the temporal retina at this point, the pattern of labeling supports the map. The retrograde labeling spread to the more central regions of the retina because the LM3 injection spread laterally in LMl (Fig. 2K), and both injections spread medially in LMm (Fig. 2K,W,X). The injection in case LM1 was similar to these

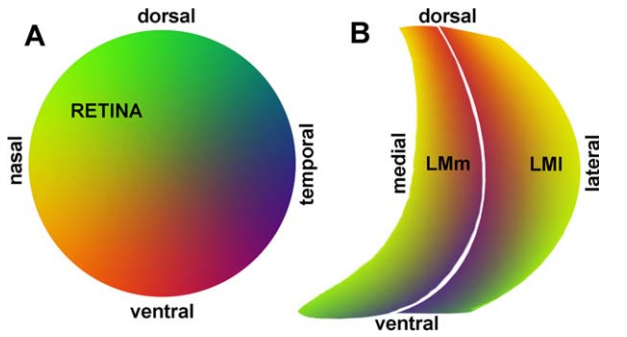

Figure 7. A retinotopic map in the medial and lateral subnuclei of the pretectal nucleus lentiformis mesencephali (LMm, LMl) based on data from Gamlin and Cohen (1988). **A:** The quadrants of the retina color-coded. This was created by stretching a green-to-red gradient along the dorsal axis, and a yellow-to-blue along the nasal-to-temporal axis. This was then stretched across the LM in **B** according to the schemed offered by Gamlin and Cohen (1988). In their scheme the nasal, temporal, dorsal, and ventral parts of the retina are represented in the dorsomedial, ventrolateral, ventromedial, and dorsolateral regions of LMm. The retinotopy in LMl is a reflection of LMm about the vertical axis.

two, perhaps slightly more dorsal. The retrograde labeling was also similar, but there was more in the central, as opposed to the temporal, retina. The retrograde labeling in cases LM/nBOR and LM/TeO were similar to that in cases LM3 and LM/DLL but more extensive. The labeling for cases LM/nBOR and LM/TeO was heaviest in the temporal retina just below the horizontal meridian, but extended to the nasal side of the central retina, and a little more dorsally than in cases LM1, LM3, and LM/DLL. The injection in case LM/nBOR was mainly in LMl, but again right on the border with LMm. From the part of injection depicted in Figure 2O, labeling would be expected in the temporal/ventral retina as the injection is on the border of LMm/l, and the centrally, nasally, and dorsally as the injection involves the middle parts of LMl. The part of the injection depicted in Figure 2N included the mediolateral extent of a piece of ventral LMl. This would result in labeling in the temporal and dorsal regions of the retina. The injection in case LM/TeO was similar to LM/nBOR, except more ventral and caudal. Less labeling (relative to case LM/nBOR) would be expected in the ventral retina, which was observed: at the level of the pecten, the density of retrograde labeling was higher for case LM/nBOR (Fig. 5D) than case LM/TeO (Fig. 5E). Moreover, with a greater involvement of the ventral LMl and LMm for the injection in case LM/TeO, the extent of the retrograde labeling would be expected to involve more of the dorsal retina. This was observed as the retrograde labeling in case LM/TeO extended dorsally into the lower parts of the red field (Fig. 5E). The

distribution of retrograde labeling in case LM2 was the most different from the others: there was less labeling in the temporal retina and more in the dorsotemporal and ventronasal regions. The bulk of the injection was quite caudomedial in LM (Fig. 2F) and the observed labeling in the dorsotemporal retina would be expected from this part of the injection. The injection spread to include the medial part of LMm and the extreme dorsal part of LMm (Fig. 2G,H), which would account for the labeling in the nasal and ventronasal retina. In summary, although the extent of the injections in the present study would be insufficient to determine the retinotopy in LM, the distribution of retrograde labeling that we observed from our injections is consistent with the retinotopy proposed by Gamlin and Cohen (1988).

Inputs to individual LM neurons

Neurons in the AOS and pretectum respond to largefield visual motion by summing inputs from local motion detectors (Ibbotson and Clifford, 2001). This has been explicitly demonstrated by Kogo et al. (1998) in the nBOR of turtles, where they determined that each nBOR neuron receives input from 12–36 ganglion cells, all preferring approximately the same direction of motion. As DGCs provide the majority of input to nBOR in pigeons, it has been assumed that each nBOR neuron would receive input from an array of DGCs (Fite et al., 1981). Given that we found that large RGCs do project to nBOR (confirming Nickla et al., 1994), this could be amended to such that each nBOR neuron receives input from an array of DGCs and perhaps a few large RGCs. For the LM the case is different and there are at least two possibilities: 1) some LM neurons receive input exclusively from RGCs, whereas others receive input exclusively from DGCs; and/or 2) individual LM neurons receive input from several RGCs and fewer DGCs. Without further research this is impossible to determine. However, given that with some of our injections the distribution of DGCs and RGCs was not completely overlapping and in some cases very few DGCs were labeled, it is likely that for some LM neurons the inputs arise solely from RGCs.

Given the possibility that in LM there may be neurons with differing types of retinal input, one might expect to find neurons with differing response properties in LM. Although the defining feature of LM neurons is that they respond to largefield stimuli, differing response types have been noted. For example, whereas most LM neurons are direction-selective, a small percentage ($<$3%) are omnidirectional, responding equally well to motion in all directions (Fu et al., 1998; Wylie and Crowder, 2000). Most neurons (about 50%) respond best to temporal-to-nasal (T-N) motion, whereas neurons preferring upward, downward, and nasal-to-temporal (N-T) motion are equally represented (Winterson and Brauth, 1985; Wylie and Frost, 1996; Fu et al., 1998; Wylie and Crowder, 2000). Wylie and Crowder (2000) and Crowder et al. (2003) noted that there was an interaction between spatiotemporal tuning and direction. About two-thirds of LM neurons were "fast" neurons, preferring drifting gratings of high temporal frequencies (TFs) and low spatial frequencies (SFs) (speed = TF/SF). The other third, of which all but one preferred T-N motion, were "slow" neurons, responding best to drifting grating of TFs and high SFs. These "slow" LM neurons preferring T-N motion are most like nBOR neurons. Crowder and Wylie (2001) and Crowder et al. (2003) showed that most (75%) nBOR cells are "slow" neurons, preferring low TFs and high SFs. Of these "slow" nBOR neurons, none preferred T-N motion; rather, they preferred upward, downward, or N-T motion. We therefore speculate that the DGCs are projecting to the neurons in the nBOR and LM that prefer "slow" largefield motion: DGCs that prefer T-N motion project to the LM, whereas DGCs that prefer upward, downward or N-T motion project to nBOR.

CONFLICT OF INTEREST

The authors have no conflict of interest.

ROLE OF AUTHORS

All authors had full access to all the data in the study and take responsibility for the integrity of the data and the accuracy of the data analysis. Study concept and design: DRW, JK, DJG, TJL, CG-I. Acquisition of data: DRW, JK, DJG, CG-I. Analysis and interpretation of data: DRW, JK. Drafting of the article: DRW. Critical revision of the article for important intellectual content: DRW, CG-I, TJL. Statistical analysis: DRW. Obtained funding: DRW. Study supervision: DRW.

LITERATURE CITED

Binggeli RL, Paule WJ. 1969. The pigeon retina: quantitative aspects of the optic nerve and ganglion cell layer. J Comp Neurol 137:1–18.

Bodnarenko SR, Rojas X, McKenna OC. 1988. Spatial organization of the retinal projection to the avian lentiform nucleus of the mesencephalon. J Comp Neurol 269: 431–447.

Bravo H, Pettigrew JD. 1981. The distribution of neurons projecting from the retina and visual cortex to the thalamus and tectum opticum of the barn owl, *Tyto alba*, and the burrowing owl, Speotyto cunicularia. J Comp Neurol 199: 419–441.

Britto LR, Hamassaki DE. 1991. A subpopulation of displaced ganglion cells of the pigeon retina exhibits substance P-like immunoreactivity. Brain Res 546:61–68.

Britto LR, Hamassaki-Britto DE. 1993. Different subsets of displaced ganglion cells in the pigeon retina exhibit

cholecystokinin-like and enkephalin-like immunoreactivities. Neuroscience 52:403–413.
Britto LR, Keyser KT, Hamassaki DE, Karten HJ. 1988. Catecholaminergic subpopulation of retinal displaced ganglion cells projects to the accessory optic nucleus in the pigeon *(Columba livia)*. J Comp Neurol 269:109–117.
Burns S, Wallman J. 1981. Relation of single unit properties to the oculomotor function of the nucleus of the basal optic root (accessory optic system) in chickens. Exp Brain Res 42:171–180.
Clarke PG, Whitteridge D. 1976. The projection of the retina, including the 'red area' on to the optic tectum of the pigeon. Q J Exp Physiol Cogn Med Sci 61:351–358.
Crowder NA, Wylie DR. 2001. Fast and slow neurons in the nucleus of the basal optic root in pigeons. Neurosci Lett 304:133–136.
Crowder NA, Dawson MR, Wylie DR. 2003a. Temporal frequency and velocity-like tuning in the pigeon accessory optic system. J Neurophysiol 90:1829–1841.
Crowder NA, Lehmann H, Parent MB, Wylie DR. 2003b. The accessory optic system contributes to the spatiotemporal tuning of motion-sensitive pretectal neurons. J Neurophysiol 90:1140–1151.
Crowder NA, Dickson CT, Wylie DR. 2004. Telencephalic input to the pretectum of pigeons: an electrophysiological and pharmacological inactivation study. J Neurophysiol 91: 274–285.
Fischer AJ, Stell WK. 1999. Nitric oxide synthase-containing cells in the retina, pigmented epithelium, choroid, and sclera of the chick eye. J Comp Neurol 405:1–14.
Fite KV, Brecha N, Karten HJ, Hunt SP. 1981. Displaced ganglion cells and the accessory optic system of the pigeon. J Comp Neurol 195:279–288.
Gamlin PD. 2006. The pretectum: connections and oculomotor related roles. Prog Brain Res 151:379–405.
Gamlin PD, Cohen DH. 1988. Retinal projections to the pretectum in the pigeon (Columba livia). J Comp Neurol 269:1–17.
Gibson JJ. 1954. The visual perception of objective motion and subjective movement. Psychol Rev 61:304–314.
Gioanni H, Rey J, Villalobos J, Dalbera A. 1984. Single unit activity in the nucleus of the basal optic root (nBOR) during optokinetic, vestibular and visuo-vestibular stimulations in the alert pigeon (Columba livia). Exp Brain Res 57:49–60.
Giolli RA, Blanks RH, Lui F. 2006. The accessory optic system: basic organization with an update on connectivity, neurochemistry, and function. Prog Brain Res 151:407–440.
Hayes BP, Holden AL. 1983. The distribution of displaced ganglion cells in the retina of the pigeon. Exp Brain Res 49: 181–188.
Ibbotson MR, Clifford CW. 2001. Interactions between ON and OFF signals in directional motion detectors feeding the not of the wallaby. J Neurophysiol 86:997–1005.
Karten H, Hodos W. 1967. A stereotaxic atlas of the brain of the pigeon (Columba livia). Baltimore, MD: Johns Hopkins Press.
Karten HJ, Fite KV, Brecha N. 1977. Specific projection of displaced retinal ganglion cells upon the accessory optic system in the pigeon (Columba livia). Proc Natl Acad Sci U S A 74:1752–1756.
Kogo N, Rubio DM, Ariel M. 1998. Direction tuning of individual retinal inputs to the turtle accessory optic system. J Neurosci 18:2673–2684.
Miceli D, Repérant J, Medina M, Volle M, Rio JP. 2006. Distribution of ganglion cells in the pigeon retina labeled via retrograde transneuronal transport of the fluorescent dye rhodamine beta-isothiocyanate from the telencephalic visual Wulst. Brain Res 1098:94–105.
Morgan B, Frost BJ. 1981. Visual response characteristics of neurons in nucleus of basal optic root of pigeons. Exp Brain Res 42:181–188.
Nakayama K. 1985. Biological image motion processing: a review. Vision Res 25:625–660.
Nalbach HO, Wolf-Oberhollenzer F, Kirschfeld K. 1990. The pigeon's eye viewed through an ophthalmoscopic microscope: orientation of retinal landmarks and significance of eye movements. Vision Res 30:529–540.
Nickla DL, Gottlieb MD, Marin G, Rojas X, Britto LR, Wallman J. 1994. The retinal targets of centrifugal neurons and the retinal neurons projecting to the accessory optic system. Vis Neurosci 1:401–409.
Pakan JMP, Graham DJ, Wylie DR. 2010. Organization of visual mossy fiber projections and the zebrin antigenic map in the vestibulocerebellum. J Comp Neurol 518:175–198.
Reiner A, Brecha N, Karten HJ. 1979. A specific projection of retinal displaced ganglion cells to the nucleus of the basal optic root in the chicken. Neuroscience 4:1679–1688.
Remy M, Güntürkün O. 1991. Retinal afferents to the tectum opticum and the nucleus opticus principalis thalami in the pigeon. J Comp Neurol 305:57–70.
Shimizu T, Karten HJ. 1993. The avian visual system and the evolution of the neocortex. In: Zeigler HP, Bischof HJ, editors. Vision, brain, and behavior in birds. Cambridge, MA: MIT Press. p 103–114.
Simpson JI. 1984. The accessory optic system. Annu Rev Neurosci 7:13–41.
Simpson JI, Giolli RA, Blanks RH. 1988. The pretectal nuclear complex and the accessory optic system. Rev Oculomot Res 2:335–364.
Westheimer G, McKee SP. 1975. Visual acuity in the presence of retinal-image motion. J Opt Soc Am 65:847–850.
Wilson M, Nacsa N, Hart NS, Weller C, Vaney DI. Regional distribution of nitrergic neurons in the inner retina of the chicken. Vis Neurosci 28:205–220.
Winship IR, Crowder NA, Wylie DR. 2006. Quantitative reassessment of speed tuning in the accessory optic system and pretectum of pigeons. J Neurophysiol 95:546–551.
Winterson BJ, Brauth SE. 1985. Direction-selective single units in the nucleus lentiformis mesencephali of the pigeon (Columba livia). Exp Brain Res 60:215–226.
Woodson W, Shimizu T, Wild JM, Schimke J, Cox K, Karten HJ. 1995. Centrifugal projections upon the retina: an anterograde tracing study in the pigeon (Columba livia). J Comp Neurol 362:489–509.
Wylie DR, Crowder NA. 2000. Spatiotemporal properties of fast and slow neurons in the pretectal nucleus lentiformis mesencephali in pigeons. J Neurophysiol 84:2529–2540.
Wylie DR, Frost BJ. 1990. The visual response properties of neurons in the nucleus of the basal optic root of the pigeon: a quantitative analysis. Exp Brain Res 82:327–336.
Wylie DR, Frost BJ. 1996. The pigeon optokinetic system: visual input in extraocular muscle coordinates. Vis Neurosci 13:945–953.